

A STOCHASTIC ALGORITHM FOR FAULT INVERSE PROBLEMS IN ELASTIC HALF SPACE WITH PROOF OF CONVERGENCE*

Darko Volkov

Department of Mathematical Sciences, WPI, Worcester, Massachusetts, USA

Email: darko@wpi.edu

Abstract

A general stochastic algorithm for solving mixed linear and nonlinear problems was introduced in [11]. We show in this paper how it can be used to solve the fault inverse problem, where a planar fault in elastic half-space and a slip on that fault have to be reconstructed from noisy surface displacement measurements. With the parameter giving the plane containing the fault denoted by \mathbf{m} and the regularization parameter for the linear part of the inverse problem denoted by C , both modeled as random variables, we derive a formula for the posterior marginal of \mathbf{m} . Modeling C as a random variable allows to sweep through a wide range of possible values which was shown to be superior to selecting a fixed value [11]. We prove that this posterior marginal of \mathbf{m} is convergent as the number of measurement points and the dimension of the space for discretizing slips increase. Simply put, our proof only assumes that the regularized discrete error functional for processing measurements relates to an order 1 quadrature rule and that the union of the finite-dimensional spaces for discretizing slips is dense. Our proof relies on trace class operator theory to show that an adequate sequence of determinants is uniformly bounded. We also explain how our proof can be extended to a whole class of inverse problems, as long as some basic requirements are met. Finally, we show numerical simulations that illustrate the numerical convergence of our algorithm.

Mathematics subject classification: 45Q05, 65J20, 60F99.

Key words: Mixed Linear and nonlinear inverse problems, Bayesian modeling, Regularization, Approximation to solutions by quadrature, Convergence of Random Variables, Elasticity equations in unbounded domains.

1. Introduction

In [11], we introduced a numerical method for mixed linear and nonlinear inverse problems. This method applies to cases where the data for the inverse problem is corrupted by noise and where for each value of the nonlinear parameter, the underlying linear problem is ill-posed. Accordingly, regularizing this linear part is required. The norm used for the regularization process has to be multiplied by a scaling parameter, also called regularization parameter, denoted by C throughout this paper. In [11], a Bayesian approach was adopted, and C was modeled as a random variable. It was shown in [11] that this approach is superior to selecting C using some standard method for linear inverse problems, such as the discrepancy principle, or the generalized cross validation. Loosely speaking, this can be explained by observing that for different values of the nonlinear parameter \mathbf{m} , these classical methods will favor different values

* Received September 30, 2020 / Revised version received January 7, 2021 / Accepted April 15, 2021 / Published online January 8, 2022 /

of C , and as a result different values of the nonlinear parameter \mathbf{m} cannot be fairly compared. Attempting to select a unique value of C for all values of \mathbf{m} leads to somehow better results, but as demonstrated in the last section of this paper, doing so pales in comparison to the method advocated in [11].

In this paper, we first derive in Section 3 a specific version of the Bayesian posterior distribution of \mathbf{m} following the method introduced in [11]. This version applies to an inverse problem in half space for the linear elasticity equations. In the direct problem, a slip field on an open surface that we will call a fault, gives rise to a displacement field. In the inverse problem, this field is measured on the plane on top of the half space at M points. The linear part of the inverse problem consists of reconstructing the slip field on the fault. The nonlinear part consists of finding the geometry and the location of the fault. This formulation is commonly used in geophysics to model slow slip events in the vicinity of subduction zones, or the total displacement resulting from a dynamic earthquake, see [13, 14] and references therein. In this paper, the geometry of the fault is assumed to be planar, thus we choose the nonlinear parameter \mathbf{m} to be in \mathbb{R}^3 . The stochastic model considered in this paper is different from a model studied in an earlier paper by the same author [12]. As explained in section 3, the difference is that we here assume the regularization parameter C for the linear part of the inverse problem to be a random variable and the covariance σ of the measurements is unknown. In section 3, the likelihood of σ is optimized based on the data and as a consequence the resulting posterior distribution function of \mathbf{m} is entirely different from the simpler one used in [12]. Computing this new posterior is more intricate since it involves the random variable (\mathbf{m}, C) instead of just \mathbf{m} in [12]. The benefit of using this new posterior is that it leads to much better numerical results if the covariance σ of the measurements is unknown as shown in sections 6.2 and 6.3.

In Section 4, we provide a mathematical proof of the soundness of our Bayesian approach for computing the posterior probability density of \mathbf{m} . More precisely, we show that as the number of measurement points M tends to infinity and the dimension of the space for discretizing slip fields tends to infinity, the probability of \mathbf{m} to be further than a fixed $\eta > 0$ from the true value $\tilde{\mathbf{m}}$ converges to zero if the noise level is low enough. Interestingly, although the derivation of the probability law of the posterior of \mathbf{m} assumes that the noise is Gaussian, once this law is set the proof of convergence does not require the noise to be Gaussian. The proof assumes that the regularized discrete error functional for sampling measurements relates to an order 1 quadrature rule for C^1 functions (which is verified by most commonly used quadrature rules) and that the union of the finite-dimensional spaces for discretizing slips is dense, a natural requirement that can be easily satisfied by combining adequate finite element spaces. The more difficult step in this proof of convergence requires showing that a sequence of determinants is uniformly bounded: this can be achieved by using trace class operator theory [6].

In Section 5, for the reader's convenience, we extend the formulation of our recovery method to more general inverse problems. We write down the expression of the posterior probability distribution that is at the core of our reconstruction method. A companion parallel sampling algorithm is given in [11], Section 3.2. At the end of Section 5 of this paper, we state a convergence theorem for the posterior probability distribution which is valid in this more general framework.

In Section 6, we present numerical simulations that use our posterior probability distribution for reconstructing the geometry parameter \mathbf{m} . The posterior marginals of \mathbf{m} and of the regularization parameter C are computed using the method of choice sampling due to the size of the search space. We used a modified version of the Metropolis algorithm which is well suited

to parallel computing, [3]. This modified version was described in details in previous work, [11]. The computed posterior marginals shown in section 6 illustrate the theoretical convergence result proved in section 4: in the low noise case, as well as in the high noise case, the posterior marginals of \mathbf{m} tighten around the true value $\tilde{\mathbf{m}}$ as the number of measurement points and the dimension of the space for discretizing slips increase, as expected from Theorem 4.1. Of course in the low noise case, the tightening is more narrow, also as expected from Theorem 4.1. In a final section, we show how using a simplistic method where different values of the regularization parameter C are first fixed and then marginal posteriors of \mathbf{m} are computed, leads to results that are impossible to interpret since there is no objective way to select an optimal C for mixed linear and nonlinear problems if the variance of the noise is unknown.

2. Governing Equations, Inverse Problem and Error Functionals

2.1. Formulation of the direct and the inverse fault problems

Using standard rectangular coordinates, let $\mathbf{x} = (x_1, x_2, x_3)$ denote elements of \mathbb{R}^3 . We define \mathbb{R}^{3-} to be the open half space $x_3 < 0$. The direct problem relies on the equations of linear elasticity with Lamé constants λ and μ such that $\lambda > 0$ and $\lambda + \mu > 0$. For a vector field $\mathcal{V} = (\mathcal{V}_1, \mathcal{V}_2, \mathcal{V}_3)$, the stress vector in the direction $\mathbf{e} \in \mathbb{R}^3$ will be denoted by

$$T_{\mathbf{e}}\mathcal{V} = \sum_{j=1}^3 (\lambda \operatorname{div} \mathcal{V} \delta_{ij} + \mu (\partial_i \mathcal{V}_j + \partial_j \mathcal{V}_i)) e_j.$$

Let Γ be a Lipschitz open surface strictly included in \mathbb{R}^{3-} with normal vector \mathbf{n} defined almost everywhere. We define the jump $[\mathcal{V}]$ of the vector field \mathcal{V} across Γ to be

$$[\mathcal{V}](\mathbf{x}) = \lim_{h \rightarrow 0^+} \mathcal{V}(\mathbf{x} + h\mathbf{n}) - \mathcal{V}(\mathbf{x} - h\mathbf{n}),$$

for \mathbf{x} in Γ , if this limit exists. Let \mathcal{U} be the displacement field solving

$$\mu \Delta \mathcal{U} + (\lambda + \mu) \nabla \operatorname{div} \mathcal{U} = 0 \quad \text{in } \mathbb{R}^{3-} \setminus \Gamma, \tag{2.1}$$

$$T_{\mathbf{e}_3} \mathcal{U} = 0 \quad \text{on the surface } x_3 = 0, \tag{2.2}$$

$$T_{\mathbf{n}} \mathcal{U} \quad \text{is continuous across } \Gamma, \tag{2.3}$$

$$[\mathcal{U}] = \mathcal{G} \quad \text{is a given jump across } \Gamma, \tag{2.4}$$

$$\mathcal{U}(\mathbf{x}) = O\left(\frac{1}{|\mathbf{x}|^2}\right), \quad \nabla \mathcal{U}(\mathbf{x}) = O\left(\frac{1}{|\mathbf{x}|^3}\right), \quad \text{uniformly as } |\mathbf{x}| \rightarrow \infty, \tag{2.5}$$

where \mathbf{e}_3 is the vector $(0, 0, 1)$. Let $\tilde{H}^{\frac{1}{2}}(\Gamma)^2$ be the space of restrictions to Γ of tangential fields in $H^{\frac{1}{2}}(\partial D)^2$ supported in $\bar{\Gamma}$, where D is a bounded domain in \mathbb{R}^{3-} such that $\Gamma \subset \partial D$. In [13], we defined the functional space \mathbf{S} of vector fields \mathcal{V} defined in $\mathbb{R}^{3-} \setminus \bar{\Gamma}$ such that $\nabla \mathcal{V}$ and $\mathcal{V}/(1+r^2)^{\frac{1}{2}}$ are in $L^2(\mathbb{R}^{3-} \setminus \bar{\Gamma})^3$ and we proved the following result.

Theorem 2.1. *Let \mathcal{G} be in $\tilde{H}^{\frac{1}{2}}(\Gamma)^2$. The problem (2.1)–(2.4) has a unique solution in \mathbf{S} . In addition, the solution \mathcal{U} satisfies the decay conditions (2.5).*

The following theorem shown in [13] asserts that \mathcal{G} and Γ are uniquely determined from the data \mathcal{U} given on a relatively open set of the plane $x_3 = 0$ if we know that Γ is planar.

Theorem 2.2. *Let Γ_1 and Γ_2 be two planar open surfaces. For i in $\{1, 2\}$, assume that \mathcal{U}^i solves (2.1)–(2.5) for Γ_i in place of Γ and \mathcal{G}^i , a tangential field in $\tilde{H}^{\frac{1}{2}}(\Gamma_i)^2$, in place of \mathcal{G} . Assume that \mathcal{G}^i has full support in Γ_i , that is, $\text{supp } \mathcal{G}_i = \overline{\Gamma}_i$. Let V be a non empty open subset in $\{x_3 = 0\}$. If \mathcal{U}^1 and \mathcal{U}^2 are equal in V , then $\Gamma_1 = \Gamma_2$ and $\mathcal{G}^1 = \mathcal{G}^2$.*

Theorems 2.1 and 2.2 were proved in [13] for media with constant Lamé coefficients and in [2] for more general Lamé systems. Similar results were obtained in [1] for layered media, albeit in a bounded domain.

The solution \mathcal{U} to problem (2.1)–(2.4) can be expressed as the convolution on Γ

$$\mathcal{U}(\mathbf{x}) = \int_{\Gamma} \mathbf{H}(\mathbf{x}, \mathbf{y}, \mathbf{n}) \mathcal{G}(\mathbf{y}) ds(\mathbf{y}), \tag{2.6}$$

where \mathbf{H} is the Green tensor associated to the system (2.1)–(2.5), and \mathbf{n} is the vector normal to Γ . The practical determination of this half space Green tensor \mathbf{H} was studied in [9] and later, more rigorously, in [10]. Due to formula (2.6) we can define a continuous mapping from tangential fields \mathcal{G} in $H_0^1(\Gamma)^2$ to surface displacement fields $\mathcal{U}(x_1, x_2, 0)$ in $L^2(V)^3$ where \mathcal{U} and \mathcal{G} are related by (2.1)–(2.5). This mapping is compact since $\mathbf{H}(\mathbf{x}, \mathbf{y}, \mathbf{n})$ is smooth for (\mathbf{x}, \mathbf{y}) in $\overline{V} \times \overline{\Gamma}$. Theorem 2.2 asserts that this compact mapping is injective, so its inverse can be defined. As the inverse of a compact mapping is unbounded, finding \mathcal{G} from $\mathcal{U}(x_1, x_2, 0)$ has to involve regularization.

2.2. A regularized functional for the reconstruction of planar faults

Let R be a bounded, non-empty, open set of the plane $x_3 = 0$. Let B be a compact set of (a, b, d) in \mathbb{R}^3 such that

$$\{(x_1, x_2, ax_1 + bx_2 + d) : (x_1, x_2) \in R\}$$

is included in the half-space $x_3 < 0$. We introduce the notations

$$\begin{aligned} \mathbf{m} &= (a, b, d), \\ \Gamma_{\mathbf{m}} &= \{(x_1, x_2, ax_1 + bx_2 + d) : (x_1, x_2) \in R\}. \end{aligned}$$

It follows that the distance between $\Gamma_{\mathbf{m}}$ and the plane $x_3 = 0$ is bounded below by the same positive constant for all \mathbf{m} in B . We assume that slips \mathcal{G} are supported in such sets $\Gamma_{\mathbf{m}}$. We can then map all these fields into the rectangle R . We thus obtain displacement vectors for \mathbf{x} in V by the integral formula

$$\mathcal{U}(\mathbf{x}, \mathcal{G}, \mathbf{m}) = \int_R \mathbf{H}_{\mathbf{m}}(\mathbf{x}, y_1, y_2) \mathcal{G}(y_1, y_2) s dy_1 dy_2, \tag{2.7}$$

for any \mathcal{G} in $H_0^1(R)^2$ and \mathbf{m} in B , where s is the surface element on $\Gamma_{\mathbf{m}}$ and $\mathbf{H}_{\mathbf{m}}(\mathbf{x}, y_1, y_2)$ is derived from the Green’s tensor \mathbf{H} for \mathbf{y} on $\Gamma_{\mathbf{m}}$. We now assume that V is a bounded open subset of the plane $x_3 = 0$. For a fixed $\tilde{\mathcal{U}}$ be in $L^2(V)$, and a fixed \mathbf{m} in B we define the regularized error functional

$$\mathcal{F}_{\mathbf{m}, C}(\mathcal{G}) = \int_V |\mathcal{U}(\mathbf{x}, \mathcal{G}, \mathbf{m}) - \tilde{\mathcal{U}}(\mathbf{x})|^2 d\mathbf{x} + C \int_R |\nabla \mathcal{G}|^2, \tag{2.8}$$

where $C > 0$ is the regularization parameter and \mathcal{G} is in $H_0^1(R)^2$. Define the operator

$$\begin{aligned} \mathcal{A}_m &: H_0^1(R)^2 \rightarrow L^2(V)^3 \\ \mathcal{G} &\rightarrow \int_R \mathbf{H}_m(\mathbf{x}, y_1, y_2) \mathcal{G}(y_1, y_2) s dy_1 dy_2. \end{aligned} \tag{2.9}$$

It is clear that \mathcal{A}_m is linear, continuous, and compact. The functional $\mathcal{F}_{m,C}$ can also be written as,

$$\mathcal{F}_{m,C}(\mathcal{G}) = \|\mathcal{A}_m \mathcal{G} - \tilde{\mathcal{U}}\|_{L^2(V)^3}^2 + C \|\mathcal{G}\|_{H_0^1(R)^2}^2, \tag{2.10}$$

where in $H_0^1(R)^2$ we use the norm

$$\|\mathcal{G}\|_{H_0^1(R)^2} = \left(\int_R |\nabla \mathcal{G}|^2 \right)^{\frac{1}{2}}. \tag{2.11}$$

In the remainder of this paper, for the sake of simplifying notations, both $\|\cdot\|_{L^2(V)^3}$ and $\|\cdot\|_{H_0^1(R)^2}$ will be abbreviated by $\|\cdot\|$; context will eliminate any risk of confusion.

Proposition 2.1. *For any fixed \mathbf{m} in B and $C > 0$, $\mathcal{F}_{m,C}$ achieves a unique minimum $\mathcal{H}_{m,C}$ in $H_0^1(R)^2$.*

Proof. This result holds thanks to classic Tikhonov regularization theory (for example, see [8], Theorem 16.4). □

For $\mathcal{H}_{m,C}$ as in the statement of Proposition 2.1 we set,

$$f_C(\mathbf{m}) = \mathcal{F}_{m,C}(\mathcal{H}_{m,C}). \tag{2.12}$$

Proposition 2.2. *f_C is a Lipschitz continuous function on B . It achieves its minimum value on B .*

Proof. This was proved in [12], Proposition 3.2. □

It is helpful to state a direct consequence of uniqueness Theorem 2.2 in terms of the operators \mathcal{A}_m .

Proposition 2.3. *Let \mathbf{m}, \mathbf{m}' be in B and $\mathcal{G}, \mathcal{G}'$ be in $H_0^1(R)^2$. Assume that \mathcal{G} or \mathcal{G}' is non-zero. If $\mathcal{A}_m \mathcal{G} = \mathcal{A}_{m'} \mathcal{G}'$ then $\mathbf{m} = \mathbf{m}'$ and $\mathcal{G} = \mathcal{G}'$.*

In the remainder of this paper, we only consider one-directional fields \mathcal{G} . Accordingly, \mathcal{G} can be considered to be a scalar function in the space $H_0^1(R)$, and \mathcal{A}_m becomes a linear operator from $H_0^1(R)$ to $L^2(V)^3$.

2.3. A functional for the reconstruction of planar faults from surface measurements at M points

For $j = 1, \dots, M$, let P_j be points in V , so on the surface $x_3 = 0$, and $\tilde{\mathbf{u}}(P_j)$ be measured displacements at these points. Let H be a finite-dimensional subspaces of $H_0^1(R)$. For \mathcal{G} in H and \mathbf{m} in B , define the functional

$$F_{m,C}(\mathcal{G}) = \sum_{j=1}^M C'(j) |(\mathcal{A}_m \mathcal{G} - \tilde{\mathbf{u}})(P_j)|^2 + C \int_R |\nabla \mathcal{G}|^2, \tag{2.13}$$

where \mathcal{A}_m was defined in (2.9), and $C > 0$ is the regularization parameter. We assume that the constants $C'(j)$ are positive.

Proposition 2.4. *The functional $F_{\mathbf{m},C}$ achieves a unique minimum on H .*

Proof. This results again from Tikhonov regularization theory. □

As $F_{\mathbf{m},C}$ achieves its minimum at some $\mathbf{h}_{\mathbf{m},C}$ in H , we set

$$f_C^{\text{disc}}(\mathbf{m}) = F_{\mathbf{m},C}(\mathbf{h}_{\mathbf{m},C}). \tag{2.14}$$

The superscript “disc” stands for discrete.

Proposition 2.5. *f_C^{disc} is a Lipschitz continuous function on B and achieves its minimum value on B .*

Proof. The proof is similar to that of Proposition 2.2. □

3. Bayesian Model Derivation

We assume in our stochastic model that the geometry parameter $\mathbf{m} = (a, b, d)$ is in B and the measurements $\tilde{\mathbf{u}}(P_j)$ are related by the equation

$$(\tilde{\mathbf{u}}(P_1), \dots, \tilde{\mathbf{u}}(P_M)) = \delta + (\mathcal{A}_{\mathbf{m}}\mathbf{g}(P_1), \dots, \mathcal{A}_{\mathbf{m}}\mathbf{g}(P_M)) + \mathcal{E}, \tag{3.1}$$

where $\mathcal{A}_{\mathbf{m}}$ is as in (2.9), \mathbf{g} is in H , and \mathcal{E} in \mathbb{R}^{3M} is additive noise, which is modeled to be a random variable. The error term δ is given by

$$(\mathcal{A}_{\mathbf{m}}(I - \Pi)(\mathcal{G})(P_1), \dots, \mathcal{A}_{\mathbf{m}}(I - \Pi)(\mathcal{G})(P_M)), \tag{3.2}$$

where Π is the orthogonal projection from $H_0^1(R)$ to H and \mathcal{G} is in $H_0^1(R)$. δ represents the part of the slip that cannot be reached by the finite dimensional model and $\mathbf{g} = \Pi\mathcal{G}$. We assume in this section that \mathcal{E} follows a normal probability distribution with mean zero and diagonal covariance matrix $\sigma^2 I$ after rescaling by C' , so altogether the diagonal of this covariance matrix is the vector in \mathbb{R}^{3M} is

$$\sigma^2(C'(1)^{-1}, C'(1)^{-1}, C'(1)^{-1}, \dots, C'(M)^{-1}, C'(M)^{-1}, C'(M)^{-1}).$$

The $3M$ dimensional vector $(\tilde{\mathbf{u}}(P_1), \dots, \tilde{\mathbf{u}}(P_M))$ will be denoted by $\tilde{\mathbf{u}}$. Given our assumption on the noise \mathcal{E} , for a fixed \mathbf{m} and \mathbf{g} the random variable $(\mathcal{A}_{\mathbf{m}}\mathbf{g}(P_1), \dots, \mathcal{A}_{\mathbf{m}}\mathbf{g}(P_M)) + \mathcal{E}$ is normal with mean $(\mathcal{A}_{\mathbf{m}}\mathbf{g}(P_1), \dots, \mathcal{A}_{\mathbf{m}}\mathbf{g}(P_M))$ and covariance $\sigma^2 I$. Accordingly, by (3.1), the probability density of $\tilde{\mathbf{u}} - \delta$ knowing the geometry parameter \mathbf{m} , the slip field \mathbf{g} and the variance σ is

$$\rho(\tilde{\mathbf{u}} - \delta | \mathbf{m}, \mathbf{g}, \sigma) \propto \exp\left(-\frac{1}{2\sigma^2} \sum_{j=1}^M C'(j) |\mathcal{A}_{\mathbf{m}}\mathbf{g} - \tilde{\mathbf{u}}|^2(P_j)\right). \tag{3.3}$$

Next, we assume that \mathbf{m} in B and \mathbf{g} in H are independent random variables. The prior distribution of \mathbf{m} , ρ_{pr} , is assumed to be uninformative, that is, $\rho_{pr}(\mathbf{m}) \propto 1_B(\mathbf{m})$. For the prior distribution of \mathbf{g} knowing C we follow the Maximum Likelihood (ML) model introduced in [4]: this is due to the fact that we consider σ^2 to be unknown. In [4], Galatsanos and Katsaggelos only studied a linear problem and later in [11], their method was extended to the case where the linear operator depends on an unknown nonlinear parameter. In that case it is advantageous

to model the regularization parameter C as a random variable [11], and the prior of \mathbf{g} is set to be,

$$\rho(\mathbf{g}|\sigma, C) \propto \exp\left(-\frac{C}{2\sigma^2}\|\mathbf{g}\|^2\right), \tag{3.4}$$

where $\|\mathbf{g}\|^2$ is given by the square of the natural norm in H_p , $\int_R |\nabla \mathbf{g}|^2$. Modeling C as a random variable makes the stochastic formulation derived in this paper entirely different from an earlier formulation derived in [12]. Indeed, in [12], section 5.4 describes an algorithm for a uniform selection of C for all values of \mathbf{m} . That algorithm was certainly an improvement over applying classic selection algorithms for C for linear problems (such as Generalized Cross Validation or the discrepancy principle), separately for each value of \mathbf{m} , which leads to inconsistent regularization demands for different values of \mathbf{m} and an overall poor numerical method. However, the algorithm proposed in [12] section 5.4, requires a good knowledge of the expected value of the magnitude of error measurements. Instead, in the model adopted here, the prior of C is free to roam over a large interval, and the data is used to compute the expected value of C . Interestingly, these two different approaches lead to entirely different formulas for posterior probability distributions. The approach adopted here leads to much better numerical results as demonstrated in Sections 6.2 and 6.3. The downside of the approach adopted here is that it adds one dimension to the stochastic variable whose distribution function is to be computed, and accordingly the computational challenge is one order of magnitude greater. This downside can be overcome by using a modified version of the Metropolis algorithm which is well suited to parallel computing [3, 11].

Set for \mathbf{g} in H_p ,

$$F_{\mathbf{m},C}^\delta(\mathbf{g}) = \sum_{j=1}^M C'(j) |(\mathcal{A}_{\mathbf{m}}\mathbf{g}) - \tilde{\mathbf{u}} + \delta(P_j)|^2 + C \int_R |\nabla \mathbf{g}|^2, \tag{3.5}$$

and let $\mathcal{A}_{\mathbf{m}}^M$ be the finite dimensional linear operator from H to \mathbb{R}^{3M} defined by

$$\mathcal{A}_{\mathbf{m}}^M \mathbf{g} = (C'(1)^{\frac{1}{2}} \mathcal{A}_{\mathbf{m}}(\mathbf{g})(P_1), \dots, C'(M)^{\frac{1}{2}} \mathcal{A}_{\mathbf{m}}(\mathbf{g})(P_M)) \tag{3.6}$$

Proposition 3.1. *Assume that $(\tilde{\mathbf{u}}(P_1), \dots, \tilde{\mathbf{u}}(P_M)) - \delta$ is not zero. As a function of σ , $\rho(\tilde{\mathbf{u}}|\mathbf{m}, \mathbf{g}, \sigma)$, the probability density of the measurement $\tilde{\mathbf{u}}$ knowing \mathbf{m}, \mathbf{g} , and σ , achieves a unique maximum at*

$$\sigma_{\max}^2 = \frac{1}{3M} F_{\mathbf{m},C}^\delta(\mathbf{g}_{\min}), \tag{3.7}$$

where \mathbf{g}_{\min} is the minimizer of $F_{\mathbf{m},C}^\delta$ over H . Fixing $\sigma = \sigma_{\max}$, the probability density of (\mathbf{m}, C) knowing $\tilde{\mathbf{u}}$ is then given, up to a multiplicative constant, by the formula

$$\rho(\mathbf{m}, C|\tilde{\mathbf{u}}) \propto \det(C^{-1}(\mathcal{A}_{\mathbf{m}}^M)' \mathcal{A}_{\mathbf{m}}^M + I)^{-\frac{1}{2}} F_{\mathbf{m},C}^\delta(\mathbf{g}_{\min})^{-\frac{3M}{2}} \rho_{pr}(\mathbf{m}, C). \tag{3.8}$$

Proof. Although a slightly different version of this proof can be found in [11], we still include it in this paper for the sake of completion. Using equation (3.1) and the probability law of \mathcal{E} , the probability density of $\tilde{\mathbf{u}}$ knowing $\mathbf{g}, \sigma, \mathbf{m}$, and C is, since $\tilde{\mathbf{u}}$ does not depend on C ,

$$\begin{aligned} \rho(\tilde{\mathbf{u}}|\mathbf{g}, \sigma, \mathbf{m}, C) &= \rho(\tilde{\mathbf{u}}|\mathbf{g}, \sigma, \mathbf{m}) \\ &= \left(\frac{1}{2\pi\sigma^2}\right)^{\frac{3M}{2}} \prod_{j=1}^M C'(j)^{\frac{3}{2}} \exp\left(-\frac{1}{2\sigma^2} \sum_{j=1}^M C'(j) |\tilde{\mathbf{u}} - \mathcal{A}_{\mathbf{m}}\mathbf{g} - \delta|^2(P_j)\right). \end{aligned} \tag{3.9}$$

Recalling (3.4),

$$\rho(\mathbf{g}|\sigma, \mathbf{m}, C) = \rho(\mathbf{g}|\sigma, C) = \left(\frac{C}{2\pi\sigma^2}\right)^{\frac{\dim H}{2}} \exp\left(-\frac{C}{2\sigma^2}\|\mathbf{g}\|^2\right), \tag{3.10}$$

since this prior is independent of \mathbf{m} . The joint distribution of $(\tilde{\mathbf{u}}, \mathbf{g})$ knowing σ, \mathbf{m}, C is related to the distribution of $\tilde{\mathbf{u}}$ knowing $\mathbf{g}, \sigma, \mathbf{m}, C$ by

$$\rho(\tilde{\mathbf{u}}, \mathbf{g}|\sigma, \mathbf{m}, C) = \rho(\tilde{\mathbf{u}}|\mathbf{g}, \sigma, \mathbf{m}, C) \left(\int \rho(\tilde{\mathbf{u}}, \mathbf{g}|\sigma, \mathbf{m}, C) d\tilde{\mathbf{u}}\right). \tag{3.11}$$

Now, $\int \rho(\tilde{\mathbf{u}}, \mathbf{g}|\sigma, \mathbf{m}, C) d\tilde{\mathbf{u}}$ is the prior probability distribution of \mathbf{g} [7], which we said was given by (3.10). Combining (3.9)–(3.11) we obtain,

$$\begin{aligned} \rho(\tilde{\mathbf{u}}|\sigma, \mathbf{m}, C) &= \int \rho(\tilde{\mathbf{u}}, \mathbf{g}|\sigma, \mathbf{m}, C) d\mathbf{g} \tag{3.12} \\ &= \left(\frac{1}{2\pi\sigma^2}\right)^{\frac{\dim H + 3M}{2}} C^{\frac{\dim H}{2}} \prod_{j=1}^M C'(j)^{\frac{3}{2}} \int \exp\left(-\frac{C}{2\sigma^2}\|\mathbf{g}\|^2 - \frac{1}{2\sigma^2} \sum_{j=1}^M C'(j)|\tilde{\mathbf{u}} - \mathcal{A}_m \mathbf{g} - \delta|^2(P_j)\right) d\mathbf{g}. \end{aligned}$$

The latter integral can be computed explicitly [12] to find

$$\begin{aligned} &\int \exp\left(-\frac{C}{2\sigma^2}\|\mathbf{g}\|^2 - \frac{1}{2\sigma^2} \sum_{j=1}^M C'(j)|\tilde{\mathbf{u}} - \mathcal{A}_m \mathbf{g} - \delta|^2(P_j)\right) d\mathbf{g} \\ &= \exp\left(-\frac{1}{2\sigma^2} F_{\mathbf{m}, C}^\delta(\mathbf{g}_{\min})\right) \left(\det\left(\frac{1}{2\pi\sigma^2}((\mathcal{A}_m^M)'\mathcal{A}_m^M + CI)\right)\right)^{-\frac{1}{2}}, \end{aligned} \tag{3.13}$$

where \mathbf{g}_{\min} minimizes $F_{\mathbf{m}, C}^\delta$ over H and \mathcal{A}_m^M was defined in (3.6). The determinant in (3.13) is of order $\dim H$ so some terms in σ in (3.13) and (4.9) simplify to obtain,

$$\left(\frac{1}{2\pi\sigma^2}\right)^{\frac{3M}{2}} C^{\frac{\dim H}{2}} \prod_{j=1}^M C'(j)^{\frac{3}{2}} \exp\left(-\frac{1}{2\sigma^2} F_{\mathbf{m}, C}^\delta(\mathbf{g}_{\min})\right) (\det((\mathcal{A}_m^M)'\mathcal{A}_m^M + CI))^{-\frac{1}{2}}, \tag{3.14}$$

which we now maximize for σ in $(0, \infty)$. Note that \mathbf{g}_{\min} does not depend on σ . As σ tends to infinity, the limit of (3.14) is clearly zero. As σ tends to zero the limit of (3.14) is again zero since $(\tilde{\mathbf{u}}(P_1), \dots, \tilde{\mathbf{u}}(P_M)) - \delta$ is not zero which implies that $F_{\mathbf{m}, C}^\delta(\mathbf{g}_{\min}) > 0$. We then take the derivative of (3.14) in σ and set it to equal to zero to find the equation

$$-3M\sigma^{-3M-1} + \sigma^{-3M}(-2)\sigma^{-3}\left(-\frac{1}{2}F_{\mathbf{m}, C}^\delta(\mathbf{g}_{\min})\right) = 0,$$

thus the value

$$\sigma_{\max}^2 = \frac{1}{3M} F_{\mathbf{m}, C}^\delta(\mathbf{g}_{\min})$$

maximizes the density $\rho(\tilde{\mathbf{u}}|\sigma, \mathbf{m}, C)$. Substituting (3.7) in (3.14) we find for this particular value of σ^2 ,

$$\rho(\tilde{\mathbf{u}}|\mathbf{m}, C) = \left(\frac{3}{2\pi e}\right)^{\frac{3M}{2}} \prod_{j=1}^M (MC'(j))^{\frac{3}{2}} (\det(C^{-1}(\mathcal{A}_m^M)'\mathcal{A}_m^M + I))^{-\frac{1}{2}} F_{\mathbf{m}, C}^\delta(\mathbf{g}_{\min})^{-\frac{3M}{2}}. \tag{3.15}$$

Since our goal is to reconstruct \mathbf{m} and C knowing $\tilde{\mathbf{u}}$ we apply Bayes' law

$$\rho(\mathbf{m}, C|\tilde{\mathbf{u}}) \propto \rho(\tilde{\mathbf{u}}|\mathbf{m}, C)\rho_{pr}(\mathbf{m}, C), \tag{3.16}$$

to obtain (3.8). □

4. Convergence Result

We prove in this section a convergence result as the dimension of H and the number of quadrature points on V , M , tend to infinity. In practice, the error term δ is unknown, only $\tilde{\mathbf{u}}$ is given: $F_{\mathbf{m},C}$ can be computed but not $F_{\mathbf{m},C}^\delta$. Note that δ tends to zero as $\dim H \rightarrow \infty$. Therefore, we will from now on consider the computable distribution function

$$\rho(\tilde{\mathbf{u}}|\mathbf{m}, C) = \left(\frac{3}{2\pi e}\right)^{\frac{3M}{2}} \prod_{j=1}^M (MC'(j))^{\frac{3}{2}} (\det(C^{-1}(\mathcal{A}_{\mathbf{m}}^M)' \mathcal{A}_{\mathbf{m}}^M + I))^{-\frac{1}{2}} F_{\mathbf{m},C}(\mathbf{g}_{\min})^{-\frac{3M}{2}}, \quad (4.1)$$

where this time \mathbf{g}_{\min} is the minimizer of $F_{\mathbf{m},C}$ over H . The resulting posterior distribution function is

$$\rho(\mathbf{m}, C|\tilde{\mathbf{u}}) \propto \rho(\tilde{\mathbf{u}}|\mathbf{m}, C)\rho_{pr}(\mathbf{m}, C). \quad (4.2)$$

Choosing the priors of \mathbf{m} and C to be independent and uniform in B and in $[C_0, C_1]$ respectively, where C_0 and C_1 are positive constants, it follows from (4.1), (4.2) that

$$\rho(\mathbf{m}|\tilde{\mathbf{u}}) \propto \left(\frac{3}{2\pi e}\right)^{\frac{3M}{2}} \prod_{j=1}^M (MC'(j))^{\frac{3}{2}} \int_{C_0}^{C_1} (\det(C^{-1}(\mathcal{A}_{\mathbf{m}}^M)' \mathcal{A}_{\mathbf{m}}^M + I))^{-\frac{1}{2}} F_{\mathbf{m},C}(\mathbf{g}_{\min})^{-\frac{3M}{2}} dC. \quad (4.3)$$

We will show that for all \mathbf{m} in B away from the true geometry parameter $\tilde{\mathbf{m}}$, the posterior marginal $\rho(\mathbf{m}|\tilde{\mathbf{u}})$ converges to zero as $M \rightarrow \infty$ and $\dim H \rightarrow \infty$.

As we shall see, to obtain convergence we are not just "adding" measurement points: this is why we now assume that there are M_n measurement points, where M_n is a strictly increasing sequence in \mathbb{N} . The measurement points are denoted in this section by $P_j^n, j = 1, \dots, M_n$ and in particular the set $\{P_j^n : j = 1, \dots, M_n\}$ is not necessarily included in the set $\{P_j^{n+1} : j = 1, \dots, M_{n+1}\}$. The coefficients C' are now denoted by $C'(j, n), j = 1, \dots, M_n$ and are required to relate to a quadrature rule, as specified below. Instead of just fixing a finite-dimensional subspace H of $H_0^1(R)$, we have to consider a sequence of finite-dimensional subspaces H_n . The operator defined in (3.6) is accordingly denoted by $\mathcal{A}_{\mathbf{m}}^n$, as M_n depends on n . We make the following assumptions on the sequence of finite subspaces H_n and on the quadrature rule on V :

- The quadrature with the weights $C'(j, n)$ and the nodes $P_j^n, j = 1, \dots, M_n$ is of order 1, more precisely for all ϕ in $C^1(\bar{V})$,

$$\left| \sum_{j=1}^{M_n} C'(j, n)\phi(P_j^n) - \int_V \phi \right| = O\left(\frac{1}{M_n}\right) \sup_V |\nabla \phi|. \quad (4.4)$$

•

$$C'(j, n) > 0 \quad \text{and} \quad C'(j, n) = O\left(\frac{1}{M_n}\right), \text{ uniformly in } j \quad (4.5)$$

•

$$H_n \subset H_{n+1} \text{ and } \bigcup_{n=1}^{\infty} H_n \text{ is dense in } H_0^1(R) \quad (4.6)$$

- The dimension of the space H_n does not grow too fast relative to the number of measurement points M_n , more precisely,

$$\dim H_n = O(M_n). \tag{4.7}$$

The existence of such spaces H_n and quadrature rules on V is trivial if, for example, R and V are polygons. H_n can be constructed from spaces of finite elements. A possible choice for defining the points P_j^n is

$$\{P_j^n : j = 1, \dots, M_n\} = \left(\frac{1}{n}\mathbb{Z}^2\right) \cap V.$$

In that case M_n is approximately equal to $n^2|V|$, where $|V|$ is the surface area of V . A natural choice for the quadrature coefficients $C'(j, n)$ is $C'(j, n) = \frac{1}{n^2}$. In general, the set of points $\{P_j^n : j = 1, \dots, M_n\}$ need not be laid on such a regular grid.

4.1. The error functions f_C^{disc} and the convergence of the arguments of their minima

Lemma 4.1. *Assume that \mathcal{H}_n converges weakly to \mathcal{H} in $H_0^1(R)$. Fix \mathbf{m} in B . Then $\mathcal{A}_{\mathbf{m}}\mathcal{H}_n - \mathcal{A}_{\mathbf{m}}\mathcal{H}$ converges uniformly to zero in V . Let \mathbf{m}_n be a sequence in B converging to \mathbf{m} . Then $\mathcal{A}_{\mathbf{m}_n}\mathcal{H}_n - \mathcal{A}_{\mathbf{m}}\mathcal{H}$ converges uniformly to zero in V .*

Proof. According to (2.9),

$$\begin{aligned} & |\mathcal{A}_{\mathbf{m}}\mathcal{H}_n(x_1, x_2) - \mathcal{A}_{\mathbf{m}}\mathcal{H}(x_1, x_2)| \\ &= \left| \int_R \mathbf{H}_{\mathbf{m}}(\mathbf{x}, y_1, y_2)(\mathcal{H}_n(y_1, y_2) - \mathcal{H}(y_1, y_2))s dy_1 dy_2 \right| \\ &\leq \sup_{\mathbf{x} \in V, (y_1, y_2) \in R} |\mathbf{H}_{\mathbf{m}}(\mathbf{x}, y_1, y_2)s| |R|^{\frac{1}{2}} \left(\int_R (\mathcal{H}_n(y_1, y_2) - \mathcal{H}(y_1, y_2))^2 dy_1 dy_2 \right)^{\frac{1}{2}}, \end{aligned} \tag{4.8}$$

and since \mathcal{H}_n converges strongly to \mathcal{H} in $L^2(V)$, the first claim is proved. To prove the second claim, it suffices to show that $\mathcal{A}_{\mathbf{m}_n}\mathcal{H}_n - \mathcal{A}_{\mathbf{m}}\mathcal{H}_n$ converges uniformly to zero. This is due to the estimate,

$$\begin{aligned} & |\mathcal{A}_{\mathbf{m}_n}\mathcal{H}_n(x_1, x_2) - \mathcal{A}_{\mathbf{m}}\mathcal{H}_n(x_1, x_2)| \\ &\leq \sup_{\mathbf{x} \in V, (y_1, y_2) \in R} |\mathbf{H}_{\mathbf{m}_n}(\mathbf{x}, y_1, y_2)s_{\mathbf{m}_n} - \mathbf{H}_{\mathbf{m}}(\mathbf{x}, y_1, y_2)s_{\mathbf{m}}| |R|^{\frac{1}{2}} \left(\int_R \mathcal{H}_n(y_1, y_2)^2 dy_1 dy_2 \right)^{\frac{1}{2}}, \end{aligned} \tag{4.9}$$

and the lemma is proved. □

Recall the definition (2.14) of the function f_C^{disc} , which through $F_{\mathbf{m}, C}$ also depends on M_n and H_n . It will be convenient in the proof of the next lemma to distinguish the indices of M and H , so they will be denoted by M_n and H_p . In addition, to clarify that f_C^{disc} depends on M_n and H_p , we will use the notation $f_{C, n, p}^{\text{disc}}$ to make the dependency explicit. We also use the standard notation $B(\tilde{\mathbf{m}}, r)$ for the open ball in \mathbb{R}^3 with center $\tilde{\mathbf{m}}$ and radius r . Roughly speaking, the following lemma expresses that if the data is coming from the true value $\tilde{\mathbf{m}}$, then for some $\eta > 0$, if we take \mathbf{m} in $B \setminus B(\tilde{\mathbf{m}}, \eta)$, the error functional $f_{C, n, p}^{\text{disc}}(\mathbf{m})$ will be larger compared to when we take \mathbf{m} close to $\tilde{\mathbf{m}}$. The statement and the proof of the lemma are rather intricate because we need this statement to be uniform as $n \rightarrow \infty$, and $C \rightarrow 0$.

Lemma 4.2. *Assume that $\tilde{\mathbf{u}}(P_j^n) = \mathcal{A}_{\tilde{\mathbf{m}}}\tilde{\mathcal{H}}(P_j^n) + \tilde{\mathcal{E}}(P_j^n)$, $j = 1, \dots, M_n$ for some $\tilde{\mathbf{m}}$ in B and $\tilde{\mathcal{H}} \neq 0$ in $H_0^1(R)$. Fix $\eta > 0$. Then there exists $C^* > 0$, such that for all C_0 in $(0, C^*)$, there*

exist $\eta' > 0$, $\epsilon > 0$, n_0 , and p_0 such that,

$$\begin{aligned} & \sup_{n > n_0, \dim_{H_p} > p_0} \sup_{C_0 \leq C \leq 2C_0, \mathbf{m} \in \overline{B(\tilde{\mathbf{m}}, \eta')} \cap B} f_{C,n,p}^{\text{disc}}(\mathbf{m}) \\ & < \inf_{n > n_0, \dim_{H_p} > p_0} \inf_{C_0 \leq C \leq 2C_0, \mathbf{m} \in B \setminus B(\tilde{\mathbf{m}}, \eta)} f_{C,n,p}^{\text{disc}}(\mathbf{m}), \end{aligned} \quad (4.10)$$

if $\sum_{j=1}^{M_n} C'(j, n) |\tilde{\mathcal{E}}(P_j^n)|^2 < \epsilon$ for $n > n_0$.

Proof. If we first prove (4.10) in the case where $\tilde{\mathcal{E}}(P_j^n) = 0$, for all $j = 1, \dots, M_n$, let $\sqrt{2\epsilon}$ be equal to

$$\begin{aligned} & \inf_{n > n_0, \dim_{H_p} > p_0} \inf_{C_0 \leq C \leq 2C_0, \mathbf{m} \in B \setminus B(\tilde{\mathbf{m}}, \eta)} \sqrt{f_{C,n,p}^{\text{disc}}(\mathbf{m})} \\ & - \sup_{n > n_0, \dim_{H_p} > p_0} \sup_{C_0 \leq C \leq 2C_0, \mathbf{m} \in \overline{B(\tilde{\mathbf{m}}, \eta')} \cap B} \sqrt{f_{C,n,p}^{\text{disc}}(\mathbf{m})}. \end{aligned}$$

Then, by the triangle inequality, the strict inequality (4.10) will still hold if $\sum_{j=1}^{M_n} C'(j, n) |\tilde{\mathcal{E}}(P_j^n)|^2 < \epsilon$ for $n > n_0$. Thus, without loss of generality, we can now assume that $\tilde{\mathcal{E}}(P_j^n) = 0$, for all $j = 1, \dots, M_n$ and $n > n_0$.

Arguing by contradiction, if (4.10) does not hold, then for a sequence C_k converging to zero we have that for all $\eta' > 0$, n_0 , and p_0 ,

$$\begin{aligned} & \sup_{n > n_0, \dim_{H_p} > p_0} \sup_{C_k \leq C \leq 2C_k, \mathbf{m} \in \overline{B(\tilde{\mathbf{m}}, \eta')} \cap B} f_{C,n,p}^{\text{disc}}(\mathbf{m}) \\ & \geq \inf_{n > n_0, \dim_{H_p} > p_0} \inf_{C_k \leq C \leq 2C_k, \mathbf{m} \in B \setminus B(\tilde{\mathbf{m}}, \eta)} f_{C,n,p}^{\text{disc}}(\mathbf{m}), \end{aligned}$$

and as $f_{C,n,p}^{\text{disc}}$ is increasing in C ,

$$\sup_{n > n_0, \dim_{H_p} > p_0} \sup_{\mathbf{m} \in \overline{B(\tilde{\mathbf{m}}, \eta')} \cap B} f_{2C_k, n, p}^{\text{disc}}(\mathbf{m}) \geq \inf_{n > n_0, \dim_{H_p} > p_0} \inf_{\mathbf{m} \in B \setminus B(\tilde{\mathbf{m}}, \eta)} f_{C_k, n, p}^{\text{disc}}(\mathbf{m}). \quad (4.11)$$

We can also assume that $\eta' = \eta_k = O(C_k^{\frac{1}{2}})$. We set $n_0 = a_k, p_0 = b_k$ where the sequences a_k and b_k are strictly increasing in \mathbb{N} . Let Π_{b_k} be the orthogonal projection on H_{b_k} . As $\Pi_{b_k} \tilde{\mathcal{H}}$ converges to $\tilde{\mathcal{H}}$ due to (4.6), $\mathcal{A}_{\tilde{\mathbf{m}}} \Pi_{b_k} \tilde{\mathcal{H}}$ converges uniformly to $\mathcal{A}_{\tilde{\mathbf{m}}} \tilde{\mathcal{H}}$ in V by Lemma 4.1. After possibly extracting a subsequence, we can assume that

$$\sup_{(x_1, x_2) \in V} |(\mathcal{A}_{\tilde{\mathbf{m}}} \Pi_{b_k} \tilde{\mathcal{H}})(x_1, x_2) - (\mathcal{A}_{\tilde{\mathbf{m}}} \tilde{\mathcal{H}})(x_1, x_2)| = O(C_k^{\frac{1}{2}}). \quad (4.12)$$

By continuity $\sup_{\mathbf{m} \in \overline{B(\tilde{\mathbf{m}}, \eta_k)} \cap B} f_{2C_k, n, p}^{\text{disc}}(\mathbf{m})$ is achieved at some \mathbf{m}_k in $\overline{B(\tilde{\mathbf{m}}, \eta_k)}$. It is also bounded above by

$$\sum_{j=1}^{M_n} C'(j, n) |(\mathcal{A}_{\mathbf{m}_k} \Pi_p \tilde{\mathcal{H}} - \mathcal{A}_{\tilde{\mathbf{m}}} \tilde{\mathcal{H}})^2(P_j^n) + 2C_k \int_R |\nabla \Pi_p \tilde{\mathcal{H}}|^2|. \quad (4.13)$$

Given that $|\mathbf{m}_k - \tilde{\mathbf{m}}| = O(C_k^{\frac{1}{2}})$, we can apply (4.5), (4.6), (4.9) and (4.12) to find that for all $n > a_k, p > b_k$,

$$\sum_{j=1}^{M_n} C'(j, n) |(\mathcal{A}_{\mathbf{m}_k} \Pi_p \tilde{\mathcal{H}} - \mathcal{A}_{\tilde{\mathbf{m}}} \tilde{\mathcal{H}})^2(P_j^n) = O(C_k).$$

It follows that the left hand side of (4.11) is $O(C_k)$, if $n_0 = a_k, p_0 = c_k$. From the right hand side of (4.11), we now claim that there exist a sequence \mathbf{m}'_k in $B \setminus B(\tilde{\mathbf{m}}, \eta)$ and a'_k and b'_k two strictly increasing sequences in \mathbb{N} , such that $f_{C_k, a'_k, b'_k}^{\text{disc}}(\mathbf{m}'_k) = O(C_k)$. $f_{C_k, a'_k, b'_k}^{\text{disc}}(\mathbf{m}'_k)$ is equal to

$$\sum_{j=1}^{M_{a'_k}} C'(j, a'_k) |(\mathcal{A}_{\mathbf{m}'_k} \mathbf{h}_k - \mathcal{A}_{\tilde{\mathbf{m}}} \tilde{\mathcal{H}})^2(P_j^{a'_k}) + C_k \int_R |\nabla \mathbf{h}_k|^2, \tag{4.14}$$

for some \mathbf{h}_k in $H_{b'_k}$. Since the quantity in (4.14) is $O(C_k)$, \mathbf{h}_k is bounded in $H_0^1(R)$, so after possibly extracting a subsequence, we may assume that it is weakly convergent to some \mathbf{h}^* in $H_0^1(R)$. Likewise, we may assume that \mathbf{m}'_k converges to some \mathbf{m}^* in $B \setminus B(\tilde{\mathbf{m}}, \eta)$. From Lemma 4.1 we can claim that,

$$\sum_{j=1}^{M_{a'_k}} C'(j, a'_k) |\mathcal{A}_{\mathbf{m}'_k} \mathbf{h}_k - \mathcal{A}_{\mathbf{m}^*} \mathbf{h}^*|^2(P_j^{a'_k})$$

converges to zero. Recalling (4.14), this shows that

$$\sum_{j=1}^{M_{a'_k}} C'(j, a'_k) |\mathcal{A}_{\mathbf{m}^*} \mathbf{h}^* - \mathcal{A}_{\tilde{\mathbf{m}}} \tilde{\mathcal{H}}|^2(P_j^{a'_k})$$

converges to zero. But this term also converges to $\int_V |\mathcal{A}_{\mathbf{m}^*} \mathbf{h}^* - \mathcal{A}_{\tilde{\mathbf{m}}} \tilde{\mathcal{H}}|^2$, contradicting the injectivity statement in Proposition 2.3 as $\|\mathbf{m}^* - \tilde{\mathbf{m}}\| \geq \eta > 0$ and $\tilde{\mathcal{H}} \neq 0$. \square

4.2. A uniformly bounded determinant

Lemma 4.3. *Fix two positive constants C_0 and C_1 such that $C_0 < C_1$. If (4.4) and (4.7) hold then the determinant $\det(C^{-1}(\mathcal{A}_{\mathbf{m}}^n)' \mathcal{A}_{\mathbf{m}}^n + I)$ is bounded below by 1 and above by a constant, for all n in \mathbb{N} , \mathbf{m} in B , and C in $[C_0, C_1]$.*

Proof. Using an orthonormal basis of H_n made of eigenvectors $\phi_1, \dots, \phi_{q_n}$ of $(\mathcal{A}_{\mathbf{m}}^n)' \mathcal{A}_{\mathbf{m}}^n$, we have the estimate

$$\det(C^{-1}(\mathcal{A}_{\mathbf{m}}^n)' \mathcal{A}_{\mathbf{m}}^n + I) \leq \exp\left(C^{-1} \sum_{j=1}^{q_n} \lambda_j\right) \leq \exp\left(C_0^{-1} \sum_{j=1}^{q_n} \lambda_j\right),$$

where $(\mathcal{A}_{\mathbf{m}}^n)' \mathcal{A}_{\mathbf{m}}^n \phi_j = \lambda_j \phi_j$ and q_n is the dimension of H_n . Let \mathbf{g} be in $H_0^1(R)$. Given the definition of $\mathcal{A}_{\mathbf{m}}$ (2.9) and that $\mathbf{H}_{\mathbf{m}}(\mathbf{x}, y_1, y_2)$ and $\partial_{x_i} \mathbf{H}_{\mathbf{m}}(\mathbf{x}, y_1, y_2), i = 1, 2$, are continuous in $\mathbf{x}, (y_1, y_2), \mathbf{m}$ in $\bar{V} \times \bar{R} \times B$, it follows that

$$\sup_{\mathbf{x} \in \bar{V}} |\mathcal{A}_{\mathbf{m}} \mathbf{g}| + \sup_{\mathbf{x} \in \bar{V}} |\nabla \mathcal{A}_{\mathbf{m}} \mathbf{g}| = O(\|\mathbf{g}\|),$$

uniformly for \mathbf{m} in B . Therefore, from (4.4), if \mathbf{g}, \mathbf{h} are in $H_0^1(R)$ such that $\|\mathbf{g}\| = \|\mathbf{h}\| = 1$,

$$\begin{aligned} & \sum_{j=1}^{M_n} C'(j, n) \mathcal{A}_{\mathbf{m}} \mathbf{g}(P_j^n) \cdot \mathcal{A}_{\mathbf{m}} \mathbf{h}(P_j^n) - \int_V \mathcal{A}_{\mathbf{m}} \mathbf{g} \cdot \mathcal{A}_{\mathbf{m}} \mathbf{h} \\ &= O\left(\frac{1}{M_n}\right) \sup_V |\nabla(\mathcal{A}_{\mathbf{m}} \mathbf{g} \cdot \mathcal{A}_{\mathbf{m}} \mathbf{h})| \\ &= O\left(\frac{1}{M_n}\right), \end{aligned} \tag{4.15}$$

uniformly for \mathbf{m} in B . But,

$$\sum_{k=1}^{q_n} \lambda_k = \sum_{k=1}^{q_n} \sum_{j=1}^{M_n} C'(j, n) \mathcal{A}_{\mathbf{m}} \phi_k(P_j^n) \cdot \mathcal{A}_{\mathbf{m}} \phi_k(P_j^n).$$

Recalling (4.7), $q_n = O(M_n)$, so by (4.15),

$$\sum_{k=1}^{q_n} \lambda_k = \sum_{k=1}^{q_n} \int_V \mathcal{A}_{\mathbf{m}} \phi_k \cdot \mathcal{A}_{\mathbf{m}} \phi_k + O(1).$$

Since \bar{R} and \bar{V} are compact and $\mathbf{H}_{\mathbf{m}}$ is smooth on $\bar{V} \times \bar{R}$, given the definition (2.9) of $\mathcal{A}_{\mathbf{m}}$, $\mathcal{A}_{\mathbf{m}}^* \mathcal{A}_{\mathbf{m}}$ is a trace class operator [6]. The term $\sum_{k=1}^{q_n} \langle \mathcal{A}_{\mathbf{m}} \phi_k, \mathcal{A}_{\mathbf{m}} \phi_k \rangle$ is bounded above by $\|\mathcal{A}_{\mathbf{m}}^* \mathcal{A}_{\mathbf{m}}\|_1 = \|\mathcal{A}_{\mathbf{m}} \mathcal{A}_{\mathbf{m}}^*\|_1$ where $\|\cdot\|_1$ is the trace class norm ([6], Theorem 3.5, Chapter IV). Thus there only remains to prove $\|\mathcal{A}_{\mathbf{m}} \mathcal{A}_{\mathbf{m}}^*\|_1$ is uniformly bounded for \mathbf{m} in B .

Recalling the definition of $\mathcal{A}_{\mathbf{m}}$ (2.9), we find that $\mathcal{A}_{\mathbf{m}} \mathcal{A}_{\mathbf{m}}^*$ can be given in integral form,

$$\begin{aligned} \mathcal{A}_{\mathbf{m}} \mathcal{A}_{\mathbf{m}}^* &: L^2(V)^3 \rightarrow L^2(V)^3 \\ \mathbf{u} &\rightarrow \int_V K_{\mathbf{m}}(\mathbf{x}, \mathbf{x}') \mathbf{u}(\mathbf{x}') d\mathbf{x}', \end{aligned}$$

where

$$K_{\mathbf{m}}(\mathbf{x}, \mathbf{x}') = \int_R \mathbf{H}_{\mathbf{m}}(\mathbf{x}, y_1, y_2) \mathbf{H}'_{\mathbf{m}}(\mathbf{x}', y_1, y_2) s^2 dy_1 dy_2.$$

Given that $K_{\mathbf{m}}$ is continuous in $(\mathbf{x}, \mathbf{x}')$, that V is bounded and $\mathcal{A}_{\mathbf{m}} \mathcal{A}_{\mathbf{m}}^*$ is trace class, we have the following explicit formula [6], Theorem 8.1, Chapter IV,

$$\text{tr} (\mathcal{A}_{\mathbf{m}} \mathcal{A}_{\mathbf{m}}^*) = \text{tr} \int_V K_{\mathbf{m}}(\mathbf{x}, \mathbf{x}) d\mathbf{x} = \text{tr} \int_V \int_R \mathbf{H}_{\mathbf{m}}(\mathbf{x}, y_1, y_2) \mathbf{H}'_{\mathbf{m}}(\mathbf{x}, y_1, y_2) s^2 dy_1 dy_2 d\mathbf{x}.$$

As $\mathbf{H}_{\mathbf{m}}(\mathbf{x}, y_1, y_2) s$ is uniformly bounded for \mathbf{x} in V , \mathbf{y} in R , and \mathbf{m} in B , the result follows. \square

4.3. Convergence of the posterior of \mathbf{m} as M_n and $\dim H_p$ tend to infinity

Theorem 4.1. *Assume that the data $\tilde{\mathbf{u}}$ is given by (3.1) with the true values $\mathbf{m} = \tilde{\mathbf{m}}$, $\mathcal{G} = \tilde{\mathcal{H}}$, $\mathbf{g} = \Pi_n \tilde{\mathcal{H}}$, and is such that the random variables $\mathcal{E}(P_j^n) \cdot \mathbf{e}_k$ where $j = 1, \dots, M_n$, $k = 1, 2, 3$, $n \in \mathbb{N}$, are independent and identically distributed with zero mean and finite covariance σ^2 . Suppose conditions (4.4)–(4.7) hold and that \mathbf{m} follows the distribution (4.3). Fix $\eta > 0$. Then there for all $C_0 > 0$ small enough there is a positive σ_0 such that if $\sigma < \sigma_0$, the probability of $\{\mathbf{m} \in B : |\mathbf{m} - \tilde{\mathbf{m}}| > \eta\}$ converges to zero as n tends to infinity.*

Proof. We note that due to (4.5) there is a positive constant α such that,

$$\sum_{j=1}^{M_n} C'(j, n) |\mathcal{E}(P_j^n)|^2 \leq \frac{\alpha}{M_n} \sum_{k=1}^3 \sum_{j=1}^{M_n} (\mathcal{E}(P_j^n) \cdot \mathbf{e}_k)^2.$$

Using the law of large numbers ([5], Theorem 1.93), $\frac{1}{M_n} \sum_{k=1}^3 \sum_{j=1}^{M_n} (\mathcal{E}(P_j^n) \cdot \mathbf{e}_k)^2$ converges almost surely to σ^2 as $n \rightarrow \infty$. Following Lemma 4.2, let $\epsilon > 0$ such that inequality (4.10) is satisfied and let σ_0 be a fixed positive number less than $\frac{\epsilon}{4\alpha}$. Then $\sum_{j=1}^{M_n} C'(j, n) |\mathcal{E}(P_j^n)|^2 < \frac{\epsilon}{4}$

almost surely as $n \rightarrow \infty$. Without loss of generality, we may assume that n is large enough so that $\sum_{j=1}^{M_n} C'(j, n) |\delta(P_j^n)|^2 < \frac{\epsilon}{4}$, since $\delta = \mathcal{A}_m(I - \Pi_n)\tilde{\mathcal{H}}$. Then almost surely, as $n \rightarrow \infty$,

$$\sum_{j=1}^{M_n} C'(j, n) |(\mathcal{E} + \delta)(P_j^n)|^2 < \epsilon.$$

Now let C^*, η', n_0, p_0 be as in the statement of Lemma 4.2 and assume that n is such that $n > n_0$ and $\dim H_n > p_0$ while $C_0 < C^*$. Let \bar{C} be such that

$$[C_0, 2C_0] \cap [C_0, C_1] = [C_0, \bar{C}].$$

According to (4.3),

$$\rho(\mathbf{m}|\tilde{\mathbf{u}}) = \mathcal{I}C_n \int_{C_0}^{C_1} (\det(C^{-1}(\mathcal{A}_m^n)' \mathcal{A}_m^n + I))^{-\frac{1}{2}} F_{\mathbf{m},C}(\mathbf{g}_{\min})^{-\frac{3M_n}{2}} dC,$$

where

$$C_n = \left(\frac{3}{2\pi e}\right)^{\frac{3M_n}{2}} \prod_{j=1}^{M_n} (M_n C'(j, n))^{\frac{3}{2}},$$

$$\mathcal{I}^{-1} = C_n \int_B \int_{C_0}^{C_1} (\det(C^{-1}(\mathcal{A}_m^n)' \mathcal{A}_m^n + I))^{-\frac{1}{2}} F_{\mathbf{m},C}(\mathbf{g}_{\min})^{-\frac{3M_n}{2}} dC d\mathbf{m}.$$

Set γ_1 to be the left hand side of (4.10) and γ_2 to be the right hand side of (4.10). According to Lemmas 4.2 and 4.3, for $n > n_0$ and $\dim H_n > p_0$,

$$\begin{aligned} \mathcal{I}^{-1} &\geq C_n O\left(\int_B \int_{C_0}^{C_1} F_{\mathbf{m},C}(\mathbf{g}_{\min})^{-\frac{3M_n}{2}} dC d\mathbf{m}\right) \\ &\geq C_n O\left(\int_{B(\tilde{\mathbf{m}}, \eta') \cap B} \int_{C_0}^{\bar{C}} F_{\mathbf{m},C}(\mathbf{g}_{\min})^{-\frac{3M_n}{2}} dC d\mathbf{m}\right) \\ &\geq C_n O\left(\int_{B(\tilde{\mathbf{m}}, \eta') \cap B} \int_{C_0}^{\bar{C}} \gamma_1^{-\frac{3M_n}{2}} dC d\mathbf{m}\right), \end{aligned}$$

thus

$$\mathcal{I} \leq C_n^{-1} O(\gamma_1^{\frac{3M_n}{2}}).$$

Now assume that \mathbf{m} is in $B \setminus B(\tilde{\mathbf{m}}, \eta)$. If C is in $[C_0, \bar{C}]$, then $F_{\mathbf{m},C}(\mathbf{g}_{\min}) \geq \gamma_2$. If C is in $[\bar{C}, C_1]$ then as $F_{\mathbf{m},C}$ is increasing in C , we still have that $F_{\mathbf{m},C}(\mathbf{g}_{\min}) \geq \gamma_2$. It follows that

$$\rho(\mathbf{m}|\tilde{\mathbf{u}}) \leq \mathcal{I}C_n O(\gamma_2^{-\frac{3M_n}{2}}) \leq O\left(\left(\frac{\gamma_1}{\gamma_2}\right)^{\frac{3M_n}{2}}\right).$$

We have found that the probability of $\mathbf{m} \in \{\mathbf{m} \in B : |\mathbf{m} - \tilde{\mathbf{m}}| > \eta\}$ is $O\left(\left(\frac{\gamma_1}{\gamma_2}\right)^{\frac{3M_n}{2}}\right)$, if \mathcal{E} satisfies $\sum_{j=1}^{M_n} C'(j, n) |\mathcal{E}(P_j^n)|^2 < \frac{\epsilon}{4}$ for $n > n_0$. As by Lemma 4.2, $0 < \frac{\gamma_1}{\gamma_2} < 1$, the proof is complete. \square

Remark 4.1. Let Ω be the underlying probability space for the measurements at the points P_j^n . Theorem 4.1 assumes that the random variables $\mathcal{E}(P_j^n) \cdot \mathbf{e}_k$, $j = 1, \dots, M_n$, $k = 1, 2, 3$, $n \in \mathbb{N}$ where M_n is increasing and tends to infinity, are independent and identically distributed.

The distribution (3.15) was constructed under the assumption that $\mathcal{E}(P_j^n)$ is Gaussian, however, once this distribution is set, this is no longer necessary for the convergence result of Theorem 4.1 to hold. In practice, Theorem 4.1 expresses that if measurements $\mathcal{E}(P_j^n)(\omega) \cdot \mathbf{e}_k, j = 1, \dots, M_n, k = 1, 2, 3, n \in \mathbb{N}$ are available, almost surely for ω in Ω , if $\sigma < \sigma_0$, the probability of $\{\mathbf{m} \in B : |\mathbf{m} - \tilde{\mathbf{m}}| > \eta\}$ is $O((\frac{\gamma_1}{\gamma_2})^{\frac{3M_n}{2}})$.

5. Extension to More General Inverse Problems

The reconstruction algorithm developed in this paper was initially designed to solve a specific fault inverse problem arising in geophysics. However, it can be used in other inverse problems where both linear and nonlinear unknowns have to be recovered. This algorithm is especially well-suited to problems where the linear part has to be regularized, but to what extent is unknown, and this lack of knowledge is made more challenging by the fact that the underlying linear operator depends on the linear unknown. This algorithm is also well-suited to problems where noise levels are considerable and as a result the maximum likelihood solution may become meaningless. The expected value of the solution and its (rather large) covariance are then more meaningful. Section 4.3 of [11] shows how this method outperforms other regularization parameter selection methods such as GCV or ML (used globally over the range of the nonlinear parameter) on such problems. The numerical simulations are considerably more involved in [11] since the nonlinear parameter there is in \mathbb{R}^6 and thus the gains made by applying the method advocated in this paper are even more dramatic.

We now write down a more general inverse problem that can efficiently be solved following the algorithm analyzed in this paper. For ease of notations, we only consider the case of scalar functions: the case of vector fields can easily be inferred from there.

5.1. Inverse problem formulation

Let R and V be two open bounded subsets of \mathbb{R}^d . Let the operator

$$\mathcal{A}_{\mathbf{m}} : L^2(R) \rightarrow L^2(V) \tag{5.1}$$

be a compact linear operator that depends continuously on \mathbf{m} , a parameter in $B \subset \mathbb{R}^q$. We assume that B is compact.

Uniqueness assumption:

For any \mathbf{m}_1 and \mathbf{m}_2 in B and any \mathcal{G}_1 and \mathcal{G}_2 in $H_0^1(R)$, if $\mathcal{A}_{\mathbf{m}_1}\mathcal{G}_1 = \mathcal{A}_{\mathbf{m}_2}\mathcal{G}_2$ in $L^2(V)$, then $\mathbf{m}_1 = \mathbf{m}_2$ and $\mathcal{G}_1 = \mathcal{G}_2$.

5.2. Related discrete inverse problem

Let $P_j, j = 1, \dots, M$ be points in V , referred to as measurement points. The discrete inverse problem consists of finding \mathbf{m} from noisy data at the points P_j . More precisely, let H be a finite-dimensional subspace of $H_0^1(R)$. We assume that the noisy data is given in the form

$$(\tilde{\mathbf{u}}(P_1), \dots, \tilde{\mathbf{u}}(P_M)) = (\mathcal{A}_{\tilde{\mathbf{m}}}\tilde{\mathcal{H}}(P_1), \dots, \mathcal{A}_{\tilde{\mathbf{m}}}\tilde{\mathcal{H}}(P_M)) + \mathcal{E}, \tag{5.2}$$

where $\tilde{\mathbf{m}} \in B, \tilde{\mathcal{H}} \in H_0^1(R)$. Note that earlier in this paper $(\mathcal{A}_{\tilde{\mathbf{m}}}\tilde{\mathcal{H}}(P_1), \dots, \mathcal{A}_{\tilde{\mathbf{m}}}\tilde{\mathcal{H}}(P_M))$ had to be split in two terms, one corresponding to the orthogonal projection $\Pi\tilde{\mathcal{H}}$ on H and the other term, δ , related to the residual $(I - \Pi)\tilde{\mathcal{H}}$. This splitting was instrumental to prove the

convergence result, but is no longer necessary to formulate the posterior distribution of \mathbf{m} or to state the convergence result. Here, \mathcal{E} is a random variable with mean zero and covariance $\sigma^2 I$. The vector $(\tilde{\mathbf{u}}(P_1), \dots, \tilde{\mathbf{u}}(P_M))$ will be denoted by $\tilde{\mathbf{u}}$.

Discrete inverse problem statement:

Assume that the sets R, V, B are known. Assume that the mapping $\mathbf{m} \rightarrow \mathcal{A}_{\mathbf{m}}$ is known. Recover \mathbf{m} from $\tilde{\mathbf{u}}$: compute its expected value and its covariance, and if possible, its marginal probability distribution functions.

Let $C'(j)$ be positive weights. For a fixed $C > 0$, a fixed \mathbf{m} in B , and \mathbf{g} in H , define the error functional

$$F_{\mathbf{m},C}(\mathbf{g}) = \sum_{j=1}^M C'(j) |(\mathcal{A}_{\mathbf{m}}\mathbf{g} - \tilde{\mathbf{u}})(P_j)|^2 + C \int_R |\nabla \mathbf{g}|^2. \tag{5.3}$$

To ease notations, it is convenient to introduce the finite-dimensional operator $\mathcal{A}_{\mathbf{m}}^M$ which is built as a slight correction of $\mathcal{A}_{\mathbf{m}}$ by the quadrature coefficients $C'(j)$:

$$\mathcal{A}_{\mathbf{m}}^M \mathbf{g} = (C'(1)^{\frac{1}{2}} \mathcal{A}_{\mathbf{m}}(\mathbf{g})(P_1), \dots, C'(M)^{\frac{1}{2}} \mathcal{A}_{\mathbf{m}}(\mathbf{g})(P_M)). \tag{5.4}$$

Define the probability distribution

$$\rho(\mathbf{m}, C | \tilde{\mathbf{u}}) \propto (\det(C^{-1}(\mathcal{A}_{\mathbf{m}}^M)' \mathcal{A}_{\mathbf{m}}^M + I))^{-\frac{1}{2}} F_{\mathbf{m},C}(\mathbf{g}_{\min})^{-\frac{M}{2}} \rho_{pr}(\mathbf{m}, C), \tag{5.5}$$

where \propto means “proportional to”, $F_{\mathbf{m},C}(\mathbf{g}_{\min})$ is the minimum of $F_{\mathbf{m},C}$ over H , and $\rho_{pr}(\mathbf{m}, C)$ is the prior distribution of (\mathbf{m}, C) (note that the exponent of $F_{\mathbf{m},C}(\mathbf{g}_{\min})$ is different from the one in formula (4.1): this is because in the case of the elasticity equation we have M measurements of three-dimensional vectors, while here we assumed that we have M scalar measurements). If we choose the priors of \mathbf{m} and C to be independent and uniform in B and in $[C_0, C_1]$ respectively, where C_0 and C_1 are positive constants, it follows from (5.5) that

$$\rho(\mathbf{m} | \tilde{\mathbf{u}}) \propto \int_{C_0}^{C_1} (\det(C^{-1}(\mathcal{A}_{\mathbf{m}}^M)' \mathcal{A}_{\mathbf{m}}^M + I))^{-\frac{1}{2}} F_{\mathbf{m},C}(\mathbf{g}_{\min})^{-\frac{M}{2}} dC. \tag{5.6}$$

Note that another typical choice for the prior distribution of C is to take it such that $\log_{10} C$ is uniformly distributed on an interval in \mathbb{R} .

Regarding the computation of $\rho(\mathbf{m}, C | \tilde{\mathbf{u}})$, as $\mathbf{m} \in B \subset \mathbb{R}^q$, if $q = 1$ then the trapezoidal rule is adequate. However, if $q \geq 3$, Markov Chain Monte Carlo techniques are called for. If a parallel computing platform is available, we recommend using the parallel sampling algorithm for inverse problems combining linear and nonlinear unknowns described in [11], or any algorithm along these lines.

5.3. Convergence of the solution to the discrete inverse problem to the unique solution of the underlying continuous problem

The convergence Theorem 4.1 can easily be extended to the more general inverse problem considered in this section. For the arguments used in the proof of Lemmas 4.1, 4.2, and 4.3 to be valid, the operator (5.1) has to be associated with an integration kernel $\mathbf{H}_{\mathbf{m}}$ such that

$$\mathcal{A}_{\mathbf{m}}\mathbf{g}(\mathbf{x}) = \int_R \mathbf{H}_{\mathbf{m}}(\mathbf{x}, \mathbf{y})\mathbf{g}(\mathbf{y})d\mathbf{y}, \tag{5.7}$$

for all \mathbf{g} in $L^2(R)$ and where \mathbf{H}_m is such that

$$(\mathbf{m}, \mathbf{x}, \mathbf{y}) \rightarrow \mathbf{H}_m(\mathbf{x}, \mathbf{y}) \text{ is continuous in } B \times \bar{V} \times \bar{R}, \tag{5.8}$$

and

$$(\mathbf{m}, \mathbf{x}, \mathbf{y}) \rightarrow \partial_{x_i} \mathbf{H}_m(\mathbf{x}, \mathbf{y}) \text{ is continuous in } B \times \bar{V} \times \bar{R}, i = 1, \dots, d. \tag{5.9}$$

We are able to prove a convergence result if the coefficients C' come from a quadrature rule satisfying (4.4)–(4.5) and if the finite-dimensional space $H = H_n$ satisfies (4.6)–(4.7). Note that if the geometries of R and V are simple enough (for examples if they are polygons), these conditions can be easily met.

Theorem 5.1. *Let the data $\tilde{\mathbf{u}}$ be given by (5.2) with the true values $\tilde{\mathbf{m}}, \tilde{\mathcal{H}}$, where \mathcal{A}_m satisfies (5.7–5.9), and \mathcal{E} a random vector such that its coordinates are independent and identically distributed with zero mean and finite covariance σ^2 . Assume that the coefficients C' come from a quadrature rule satisfying (4.4)–(4.5) and consider a sequence of finite-dimensional spaces H satisfying (4.6)–(4.7). Fix a distance $\eta > 0$. Then there for all $C_0 > 0$ small enough there is a positive σ_0 such that if $\sigma < \sigma_0$, the probability of $\{\mathbf{m} \in B : |\mathbf{m} - \tilde{\mathbf{m}}| > \eta\}$ under the distribution given by (5.6) converges to zero as M and $\dim H$ tend to infinity.*

6. Numerical Simulations

6.1. Construction of data

We consider data generated in a configuration closely related to studies involving field data for a particular region and a specific seismic event [12, 14]. To ensure that we perform a simulation with realistic orders of magnitude, the scaling is such that the unit for \mathbf{x} in \mathbb{R}^3 is in kilometers, while $\tilde{\mathbf{u}}$ and \mathbf{g} in (3.1) are in meters, as in [14]. For lower values of M we will use a pattern of measurement points $P_j, j = 1, \dots, M$ derived from the locations of in-situ measurement apparatus as set up by geophysicists [14]. For generating forward data we pick the particular value

$$\tilde{\mathbf{m}} = (-0.12, -0.26, -14). \tag{6.1}$$

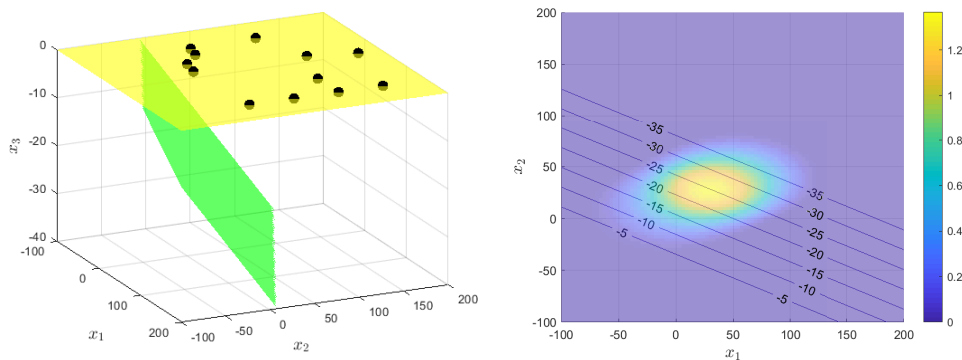


Fig. 6.1. Left: the fault $\Gamma_{\tilde{\mathbf{m}}}$ in green and the surface measurement points P_j (sketched as black dots on the plane $x_3 = 0$ which is itself shown in yellow) in the case where $M = 12$. Right: the slip \mathcal{G} on $\Gamma_{\tilde{\mathbf{m}}}$ viewed from above. \mathcal{G} is taken to be in the direction of steepest descent, so only the magnitude is shown. Depth lines on Γ_m are shown.

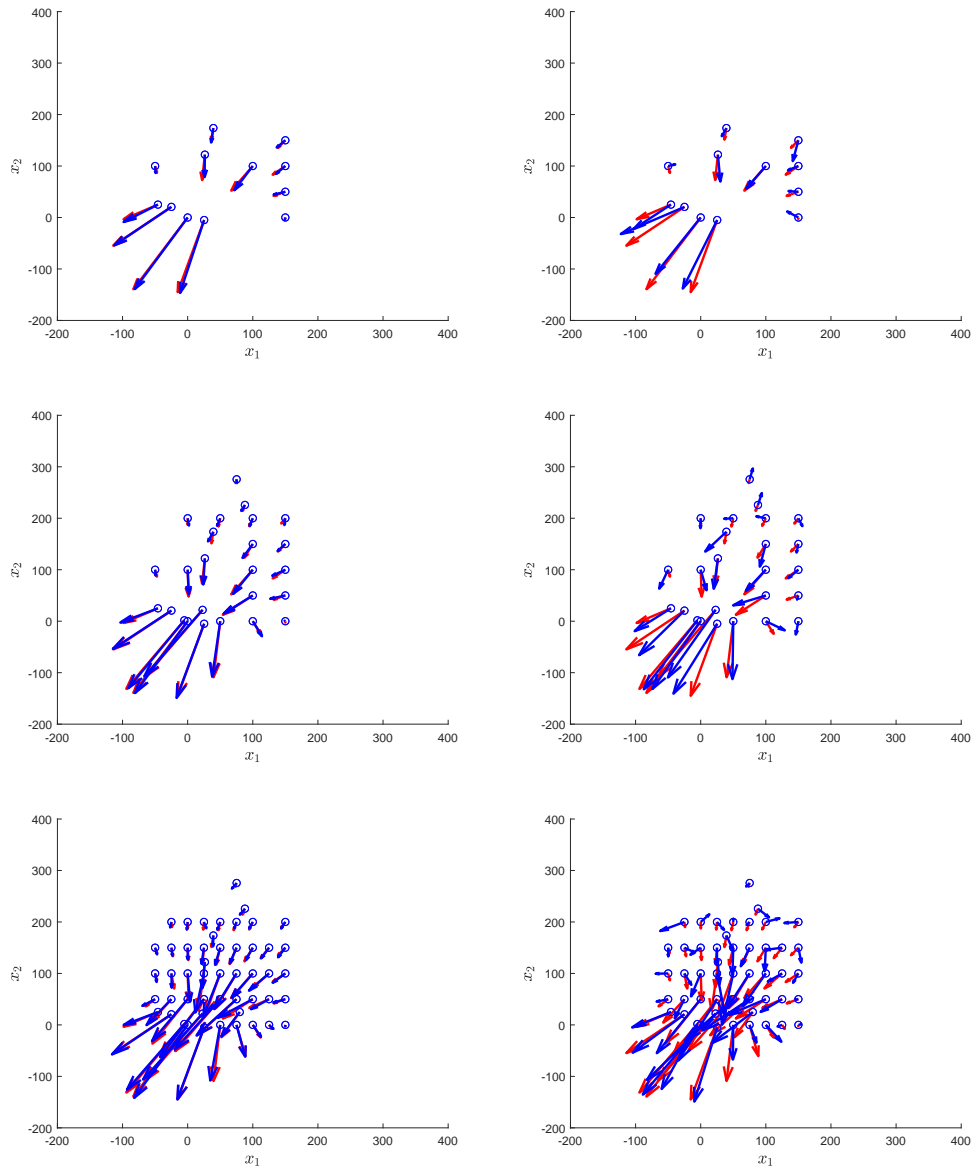


Fig. 6.2. The data $\tilde{\mathbf{u}}$ at the points P_j (represented as circles) for the six inverse problem solved numerically in this paper. Only the horizontal displacements are sketched for clarity. Row 1 to 3: $M = 12, 25, 50$. Column 1: low σ , column 2: high σ .

We sketched $\Gamma_{\tilde{\mathbf{m}}}$ in Fig. 6.1, left, where we also show the points P_j . The slip field is assumed to be parallel to the steepest direction on $\Gamma_{\tilde{\mathbf{m}}}$ and we assume that this is known when we solve the related inverse problem. This direction of slip is characteristic of plate interface in subduction zones. The slip field \mathcal{G} used for generating data as formulated by (3.1)–(3.2) is shown in Fig. 6.1, right. A very fine grid was used for computing the resulting displacement $\tilde{\mathbf{u}}$. The data for the inverse problem is the three dimensional displacements at the measurement points shown in Fig. 6.2 to which we added Gaussian noise with covariance $\sigma^2 I$. We present in this paper results for two values of σ , and for each value of σ three values of $(M, \dim H)$: $(12, 27^2)$, $(25, 37^2)$, $(50, 51^2)$.

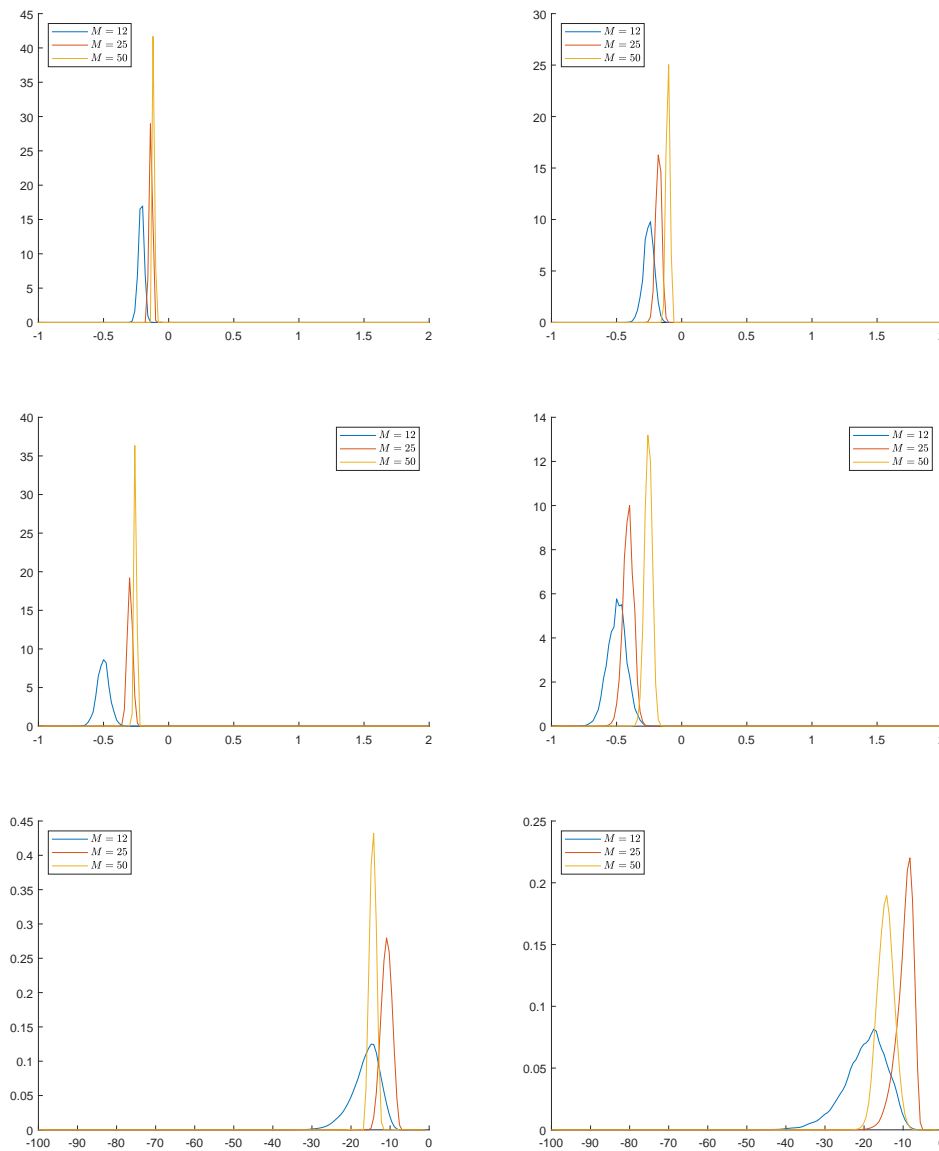


Fig. 6.3. The marginal posteriors of a, b, d computed from the data shown in Figure 6.2 in each of the six cases. Row 1, 2, 3: a, b, d . Left column: low noise case. Right column: high noise case. In each figure, the computed posterior for $M = 12, 25$, and 50 are sketched.

In the lower noise case, σ was set to be equal to 5% of the maximum of the absolute values of the components of \mathbf{u} (in other words, 5% of $\|\tilde{\mathbf{u}}\|_\infty$). For the particular realization used in solving the inverse problem, this led to a relative error in Euclidean norm of about 6%. In the higher noise case scenario σ was set to be equal to 25% of the maximum of the absolute values of the components of \mathbf{u} (in other words, 25% of $\|\tilde{\mathbf{u}}\|_\infty$) and this led to a relative error in Euclidean norm of about 30%. Both realizations are shown in Fig. 6.2 (only the horizontal components are sketched for the sake of brevity).

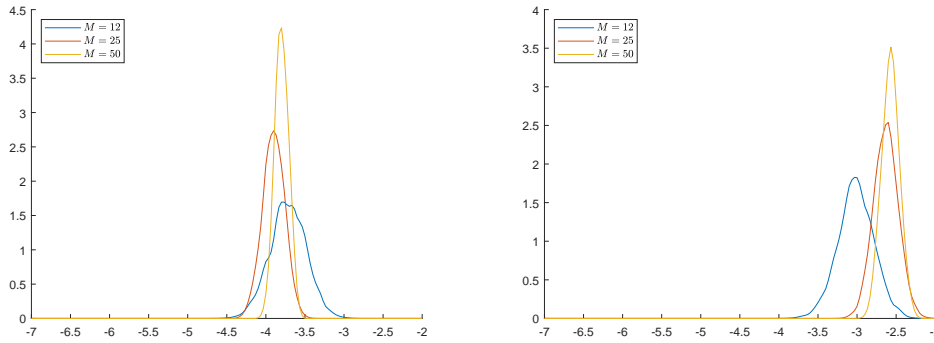


Fig. 6.4. The computed marginal posteriors of the regularization parameter C . Left: low noise case. Right: high noise case.

6.2. Numerical solution to the inverse problem

We computed the posterior probability distribution function $\rho(\mathbf{m}, C|\tilde{\mathbf{u}})$ given by (4.1)–(4.2) in each of the 6 cases introduced in the previous section. The prior distribution of \mathbf{m} was taken to be uniform in the box $[-1, 2] \times [-1, 2] \times [-100, -1]$, and the prior distribution of $\log_{10} C$ was taken to be uniform in $[-7, -2]$. The computation of $\rho(\mathbf{m}, C|\tilde{\mathbf{u}})$ was performed using the method of choice sampling, more specifically, we used a modified version of the Metropolis algorithm which is well suited to parallel computing [3]. In [11], section 4, we wrote explicitly a form of this algorithm for computing $\rho(\mathbf{m}, C|\tilde{\mathbf{u}})$. Note that although the inverse problem considered in [11] was similar to the one studied here, the nonlinear parameter to be reconstructed was different.

The computed marginal posteriors of $\mathbf{m} = (a, b, d)$ are graphed in Fig. 6.3. This figure shows how these computed posteriors tighten around the value of $\tilde{\mathbf{m}}$ as M and $\dim H$ increase as expected from Theorem 4.1. This tightening around the correct value occurs in both low and high σ cases and is more narrow in the lower noise case. Deciding that the regularization parameter C be a random variable results in a more extensive random walk, however it has the distinct advantage of sweeping through the entire range of values of C in the support of the prior of C . The computed marginal posteriors of C are sketched in Fig. 6.4. This figure illustrates how the algorithm automatically favors optimal values for C depending on M , $\dim H$, and the noise level.

6.3. Failure at fixed C

Fixing a value for the regularization parameter C is commonly done in linear inverse problems. Often times, a value for C is fixed in such a way that the solution displays satisfactory qualitative features. $\log_{10} C$ is varied linearly until such features appear. Alternatively, one can use more objective criteria for selecting C such as the maximum likelihood method, the discrepancy principle, or the generalized cross validation criterion. However, the fault inverse problem is nonlinear in \mathbf{m} . If one were to apply any of these methods to select a fixed C , the selection would depend on \mathbf{m} and as a result different candidates for \mathbf{m} would be unfairly compared, [11]. Better results are obtained if we fix the same value for C for all \mathbf{m} in B , [12]. Even then, determining the optimal value for C is not possible. To illustrate this point, we plotted in Fig. 6.5 the computed posterior marginals assuming various fixed values of the regularization

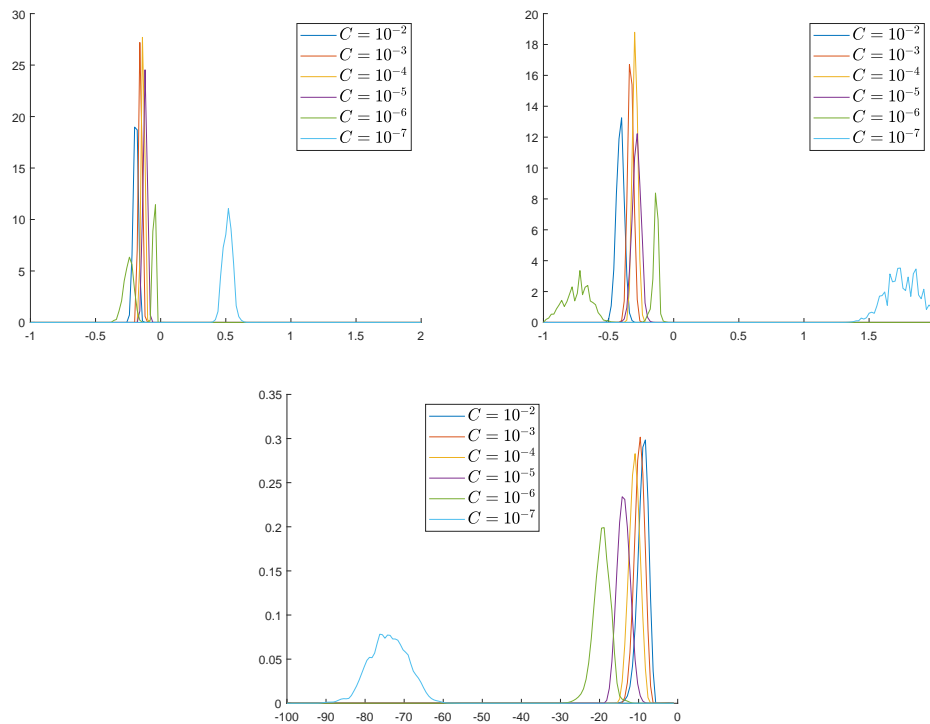


Fig. 6.5. Computed posterior marginals assuming various fixed values of the regularization parameter C . First row: a, b . Second row: d . The computed marginals are only shown for the case $M=25$, low σ .

parameter C . Qualitatively, it appears that the values 10^{-7} and 10^{-6} have to be rejected, but it is unclear which of the remaining values is most suitable. This example illustrates that modeling C as a random variable and using a Bayesian approach built from the distribution function (4.1)–(4.2) leads to far superior results.

Acknowledgments. This work was supported by Simons Foundation Collaboration Grant [351025].

References

- [1] A. Aspri, E. Beretta, and A.L. Mazzucato, Dislocations in a layered elastic medium with applications to fault detection, *arXiv preprint arXiv:2004.00321*, 2020.
- [2] A. Aspri, E. Beretta, A.L. Mazzucato, and V. Maarten, Analysis of a model of elastic dislocations in geophysics, *Archive for Rational Mechanics and Analysis*, **236**:1 (2020), 71–111.
- [3] B. Calderhead, A general construction for parallelizing metropolis-hastings algorithms, *Proceedings of the National Academy of Sciences*, **111**:49 (2014), 17408–17413.
- [4] N.P. Galatsanos and A.K. Katsaggelos, Methods for choosing the regularization parameter and estimating the noise variance in image restoration and their relation, *IEEE Transactions on image processing*, **1**:3 (1992), 322–336.
- [5] V. Girardin and N. Limnios, Applied probability, *From Random Sequences to Stochastic Processes (e-book, Springer, Cham)*, 2018.

- [6] I. Gohberg, S. Goldberg, and N. Krupnik, Traces and determinants of linear operators, *Integral Equations and Operator Theory*, **116**, Birkhäuser, 2012.
- [7] J. Kaipio and E. Somersalo, *Statistical and computational inverse problems*, Springer Science & Business Media, **160** (2006).
- [8] R. Kress, V. Maz'ya, and V. Kozlov, *Linear Integral Equations*, **17**, Springer, 1989.
- [9] Y. Okada, Internal deformation due to shear and tensile faults in a half-space. *Bulletin of the Seismological Society of America*, **82**:2 (1992), 1018–1040.
- [10] D. Volkov, A double layer surface traction free green's tensor, *SIAM Journal on Applied Mathematics*, **69**:5 (2009), 1438–1456.
- [11] D. Volkov, A parallel sampling algorithm for inverse problems with linear and nonlinear unknowns, *arXiv preprint arXiv:2007.05347*, 2020.
- [12] D. Volkov and J.C. Sandiumenge, A stochastic approach to reconstruction of faults in elastic half space, *Inverse Problems & Imaging*, **13**:3 (2019), 479–511.
- [13] D. Volkov, C. Voisin, and I.R. Ionescu, Reconstruction of faults in elastic half space from surface measurements, *Inverse Problems*, **33**:5 (2017).
- [14] D. Volkov, C. Voisin, and I.R. Ionescu, Determining fault geometries from surface displacements, *Pure and Applied Geophysics*, **174**:4 (2017), 1659–1678.